Original article

Spike-associated networks and intracranial electrographic findings[*]

Joshua J. Bear [1,2], Heidi E. Kirsch [3,4], Brian D. Berman [5], Kevin E. Chapman [1,2], Jason R. Tregellas [6,7]

[1] Department of Pediatrics, Section of Neurology, Children's Hospital Colorado, Aurora,
[2] Department of Pediatrics, University of Colorado Anschutz Medical Campus, Aurora,
[3] Department of Radiology and Biomedical Imaging, University of California, San Francisco,
[4] Department of Neurology, University of California, San Francisco,
[5] Department of Neurology, University of Colorado Anschutz Medical Campus, Aurora,
[6] Department of Psychiatry, University of Colorado Anschutz Medical Campus, Aurora,
[7] Research Service, Rocky Mountain Regional VA Medical Center, Aurora, USA

ABSTRACT – *Aims.* Functional connectivity is providing new insights into the network nature of epilepsy with growing clinical applications. Our objective was to validate a novel magnetoencephalography-based method to non-invasively measure the epileptic network.

Methods. We retrospectively identified pediatric and adult patients with refractory focal epilepsy who underwent pre-surgical magnetoencephalography with subsequent intracranial electrographic monitoring. Magnetoencephalography tracings were visually reviewed, and interictal epileptiform discharges ("spikes") were individually marked. We then evaluated differences in whole-brain connectivity during brief epochs preceding the spikes and during the spikes using the Network-Based Statistic to test differences at the network level.

Results. In six patients with statistically-significant network differences, we observed substantial overlap between the spike-associated networks and electrographically active areas identified during intracranial monitoring (the spike-associated network was 78% and 83% sensitive for intracranial electroencephalography-defined regions in the irritative and seizure onset zones, respectively).

Conclusion. These findings support the neurobiological validity of the spike-associated network method. Assessment of spike-associated networks has the potential to improve surgical planning in epilepsy surgery patients by identifying components of the epileptic network prior to implantation.

Key words: magnetoencephalography, functional connectivity, intracranial electroencephalography, epilepsy

Correspondence:
Joshua J. Bear
13123 East 16th Avenue,
Box B-155, Aurora,
CO 80045, USA
<joshua.bear@ucdenver.edu>

[*]Preliminary findings from the results presented in this manuscript were presented at the 2019 Annual Meeting of the American Clinical Neurophysiology Society.

For the 30% of individuals with focal-onset epilepsy refractory to medical therapy, at least a quarter are estimated to be curable with epilepsy surgery (Engel, 2001). The benefits of epilepsy surgery with respect to quality of life, reduced mortality, and economics have been repeatedly demonstrated (Malmgren and Edelvik, 2017). The likelihood of seizure freedom after surgery, however, is highly variable and dependent on a number of clinical factors. For the most straightforward epilepsy surgery candidates, those with seizures arising from the mesial temporal lobe and mesial temporal sclerosis on MRI, up to 80% will achieve seizure freedom (Malmgren and Edelvik, 2017). In other focal epilepsy syndromes such as MRI-negative frontal lobe epilepsy, seizure freedom rates are as low as 30% (Malmgren and Edelvik, 2017). Functional connectivity and its associated network analysis methods are emerging as powerful tools with the potential to improve our understanding of the variability in epilepsy comorbidities and surgical outcomes (Bernhardt *et al.*, 2015; Jin *et al.*, 2015).

Functional connectivity is the inferred relationship between two anatomic regions based on their covarying neuronal activity. Functional connectivity can be measured from several different neuroimaging and neurophysiology modalities including functional MRI, both scalp and invasive electroencephalography (EEG), and magnetoencephalography (MEG). MEG is a useful neuroimaging tool in presurgical evaluations in epilepsy surgery. MEG's clinical applications, however, have been largely confined to localizing the source of interictal epileptiform discharges ("spikes"). In the past several years, new analytical methods have demonstrated MEG's potential for the study of epileptic networks (Englot *et al.*, 2015). In this paper, we report on promising early findings of a new method to identify the functional epileptic network in surgical epilepsy patients using the high temporal resolution of MEG.

Methods

Patient enrollment

All individuals at the University of Colorado and Children's Hospital Colorado who underwent MEG recording for a presurgical epilepsy work-up and who subsequently had stereotactic electroencephalography (SEEG) monitoring from July 1st, 2017 to Dec 31st, 2018, were considered for inclusion. Individuals were excluded if visual review of the MEG revealed inadequate quality of the recording or fewer than five spikes per American Clinical Magnetoencephalography Society guidelines (Bagić *et al.*, 2011). Medical records review and neurophysiology data analyses were performed with the approval of the Colorado

Multiple Institutional Review Board. Source localization from the MEG data using single equivalent current dipole modeling was employed in the presurgical evaluation of all patients. The subsequent network analyses described in the following sections were performed after SEEG monitoring was complete as part of this retrospective study.

Data acquisition and preprocessing

MEG data were obtained using a Magnes 3600 WH whole-head MEG device (4D Neuroimaging, San Diego, CA, USA), comprised of 248 first-order axial-gradiometer sensors (5-cm baseline) in a magnetically shielded room (ETS-Lindgren, Cedar Park, TX, USA). Five head position indicator coils attached to the subject's scalp were used to determine the head position with respect to the sensor array. The locations of the coils with respect to three anatomical landmarks (nasion and preauricular points, with the intersection of the tragus and daith of the ear defining the preauricular points) and two extra non-fiducial points as well as the scalp surface (approximately 500 points) were determined with a 3D digitizer (Polhemus, Colchester, VT, USA). The MEG signals were acquired continuously in a 0.1-100-Hz bandwidth and sampled at 290.64 Hz and 24-bit quantization. Anatomic T1-weighted MRI scans were obtained for clinical purposes on MRI scanners at two separate locations (Children's Hospital Colorado and UCHealth at the University of Colorado) and used for co-registration and source localization. SEEG electrodes were stereotactically implanted using an image-guided system. The locations and total number of SEEG electrodes were tailored to each patient according to his or her presurgical evaluation and multidisciplinary epilepsy surgery conference discussions. Intracranial data were recorded at a minimum sampling rate of 512 Hz using 8-to-16-contact electrodes. Visual analyses of SEEG data, including identification of the irritative zone (IZ; spike-generating brain tissue) and the seizure onset zone (SOZ), were performed during routine clinical practice at each site.

Source reconstruction and estimation of the spike-associated network

MEG and MRI data were imported into MNE-Python v0.18.1 (Gramfort *et al.*, 2013) for offline processing. A trained clinical magnetoencephalographer (JJB.) visually reviewed all MEG recordings. Noisy channels were visually identified and excluded from further analysis. Spikes were manually marked for each subject starting approximately 0-25 ms prior to the spike upslope. Spikes were included only if they were preceded by a minimum three-second spike-free interval. For each subject, a group of one-second baseline epochs

starting 1.05 seconds prior to the spike marks (PRE) and a group of one-second spike-containing epochs starting at the spike marks (SPIKE) were extracted from the continuous time series data. The epochs were band-pass filtered from 12-30 Hz corresponding to the beta band. This frequency band preserves the predominant spike activity, which is by definition ≤ 70 ms in duration and has a favorable signal-to-noise ratio compared to higher frequency bands. Additionally, a minimum of 12 oscillations within the one-second time windows balances reliability of the measure with a high temporal sensitivity, as has been shown for coherence-based connectivity metrics (Sun et al., 2012).

MRI and MEG data were co-registered in the patient's anatomic space in MNE-Python. For each spike-containing epoch, source activity was estimated using standardized low-resolution brain electromagnetic tomography (sLORETA) constrained to cortical surfaces (Pascual-Marqui, 2002). The source-reconstructed data were then morphed to FreeSurfer's fsaverage brain (Reuter et al., 2012) and parcellated using the Human Connectome Project's Multimodal Parcellation (HCPMMP) (Glasser et al., 2016) consisting of 362 regions of interest (ROIs). The time course data were extracted for each parcel, and these time courses were used to generate whole-brain connectivity matrices for each PRE and SPIKE epoch. Connectivity strength was calculated using the absolute value of the imaginary component of coherence. The imaginary component of coherence is a common connectivity measure in MEG research because it removes zero-time lag correlations, which usually represent environmental artifacts and spatial leakage of inferred sources (Colclough et al., 2016).

Statistical analysis

Connectivity matrices from all PRE and SPIKE epochs were imported into the Network-Based Statistic (Zalesky et al., 2010) (NBS; v1.2) toolbox in MATLAB (R2018B). NBS compares network structure between two groups using permutation testing to determine the likelihood of finding a network of a given size after random re-organization. Many methods of comparing cortical networks operate at the level of individual node or edge features rather than at the whole network. By examining connectivity patterns at the network level, NBS is able to identify significant network differences even when some connections within the network would be too weak to be identified using other methods. NBS relies on a user-defined statistical threshold of the network graphs of interest. NBS tests were performed across a range of thresholds starting at t=2 and increasing in increments of 0.5 until no connections survived thresholding (maximum t-values ranged from 3.5 to 5 across subjects). A network difference

between the PRE and SPIKE conditions was considered significant if NBS-based permutation testing indicated that the likelihood of identifying a network of a given size at a given threshold by chance alone was less than 5% ($p < 0.05$). For visualization purposes and preliminary anatomic comparisons, graph density thresholds for each individual patient were selected to yield graphs encompassing approximately 15% of the brain, or about 50 connections between the 362 ROIs in the HCPMMP. Networks of this size were large enough to include the IZ and adjacent tissue expected to be involved in propagation on visual review, and approximated the spatial extent and distribution captured during standard clinical SEEG at the first author's institution. In order to compare the results with findings from routine clinical practice, the anatomic distribution of the MEG-based spike-associated network was compared to the visually identified IZ and SOZ on SEEG.

Results

Thirteen subjects, eight adults and five children, met the initial inclusion criteria. Four of the adults were excluded due to an inadequate number of spikes. Nine individuals underwent subsequent network analysis (table 1). In six individuals (three adults and three children), a statistically significant spike-associated network (SAN) was identified (table 2). For these subjects, the SAN was significant in all cases at all t-statistic thresholds (supplementary table 1). The three individuals in whom a significant SAN could not be identified had <30 spikes. The only two individuals in the cohort with tuberous sclerosis were included in this group, though the clinical significance of this is uncertain. One third of the cohort was female. Gender did not appear to influence the detection of a SAN, although this study was not powered to detect such a difference. In the six cases with a significant SAN, only one of whom had <30 spikes, nodes of the SAN overlapped with most or all of the anatomic regions in the SEEG-identified IZ and SOZ (table 2). Specifically, of 29 anatomic regions identified as part of the IZ among the six individuals, 21 were included in the SANs, yielding a sensitivity of 78%. Similarly, of the 20 anatomic regions identified as part of the SOZ among the six individuals, 16 were included in the SANs for a sensitivity of 83%. An illustrative case is shown in figure 1A-E. Determining an accurate specificity of the SAN method is more challenging. While the SAN consistently included areas that were not identified as part of the IZ or the SOZ by SEEG, most of the areas were not monitored during the intracranial recordings. If only those false positive nodes on the SAN, that were monitored by SEEG, were included, the overall specificity of the method in this cohort was 84%. On the other hand, if one assumes

Table 1. Subject demographics, clinical characteristics, and spike-associated network identification.

Subject	Age	Sex	Seizure type	Epilepsy etiology	No. of IEDs	Sig. SAN Identified (*p*†)
1	37	F	Focal impaired awareness seizure with non-motor symptoms (behavior arrest, autonomic)	Focal right temporal lobe epilepsy due to structural etiology (pathology consistent with focal Rasmussen's encephalitis)	52	Yes (<0.001 - 0.012)
2	12	M	Focal impaired awareness seizure with motor symptoms (tonic)	Focal epilepsy due to presumed structural etiology s/p temporal lobectomy with ongoing seizures	50	Yes (<0.001)
3	44	M	Focal impaired awareness seizure with non-motor symptoms (behavior arrest)	Focal epilepsy due to presumed structural etiology (MRI-negative)	17	Yes (<0.001 - 0.012)
4	26	M	Focal impaired awareness seizure with non-motor symptoms (sensory, autonomic)	Focal epilepsy due to presumed structural etiology (MRI-negative)	30	Yes (<0.001 - 0.026)
5	16	M	Focal aware seizure with motor symptoms (tonic, automatisms)	Focal epilepsy due to presumed structural etiology (MRI-negative)	47	Yes (<0.001)
6	17	F	Focal aware seizure with motor and non-motor symptoms (tonic, cognitive)	Focal epilepsy due to presumed structural etiology (MRI-negative)	115	Yes (<0.001)
7	19	M	Focal impaired awareness seizure with motor symptoms (tonic, automatisms)	Focal left temporal lobe epilepsy due to presumed structural etiology (focal volume loss on MRI)	6	No
8	10	M	Focal aware seizure with motor and non-motor symptoms (tonic, autonomic)	Focal structural epilepsy due to tuberous sclerosis	24	No
9	6	F	Focal impaired awareness seizure with motor and non-motor symptoms (tonic, cognitive, emotional)	Focal structural epilepsy due to tuberous sclerosis	29	No

IEDs: interictal epileptiform discharges; SAN: spike-associated network; MRI: magnetic resonance imaging.
†NBS p-value ranges for t-statistic thresholds from 2 to the highest threshold at which at least 5 nodes were part of the network in increasing intervals of 0.5

that unmonitored regions were truly not part of the IZ and/or SOZ, and therefore falsely positive when identified as part of the SAN, the specificity dropped to 67%. In considering the potential effect of spike propagation from deeper sources, a separation of 50 ms between the PRE and SPIKE conditions was thought to be adequate given evidence that propagation appears to occur within 30 ms (Zumsteg *et al.*, 2006). To confirm that the increased connectivity observed during the SPIKE condition did not precede the marked spikes, however, we performed a network comparison between the PRE condition and a 5sPRE condition (5 seconds before the IED). There were no statistically significant network increases between these time periods (*supplementary table 2*).
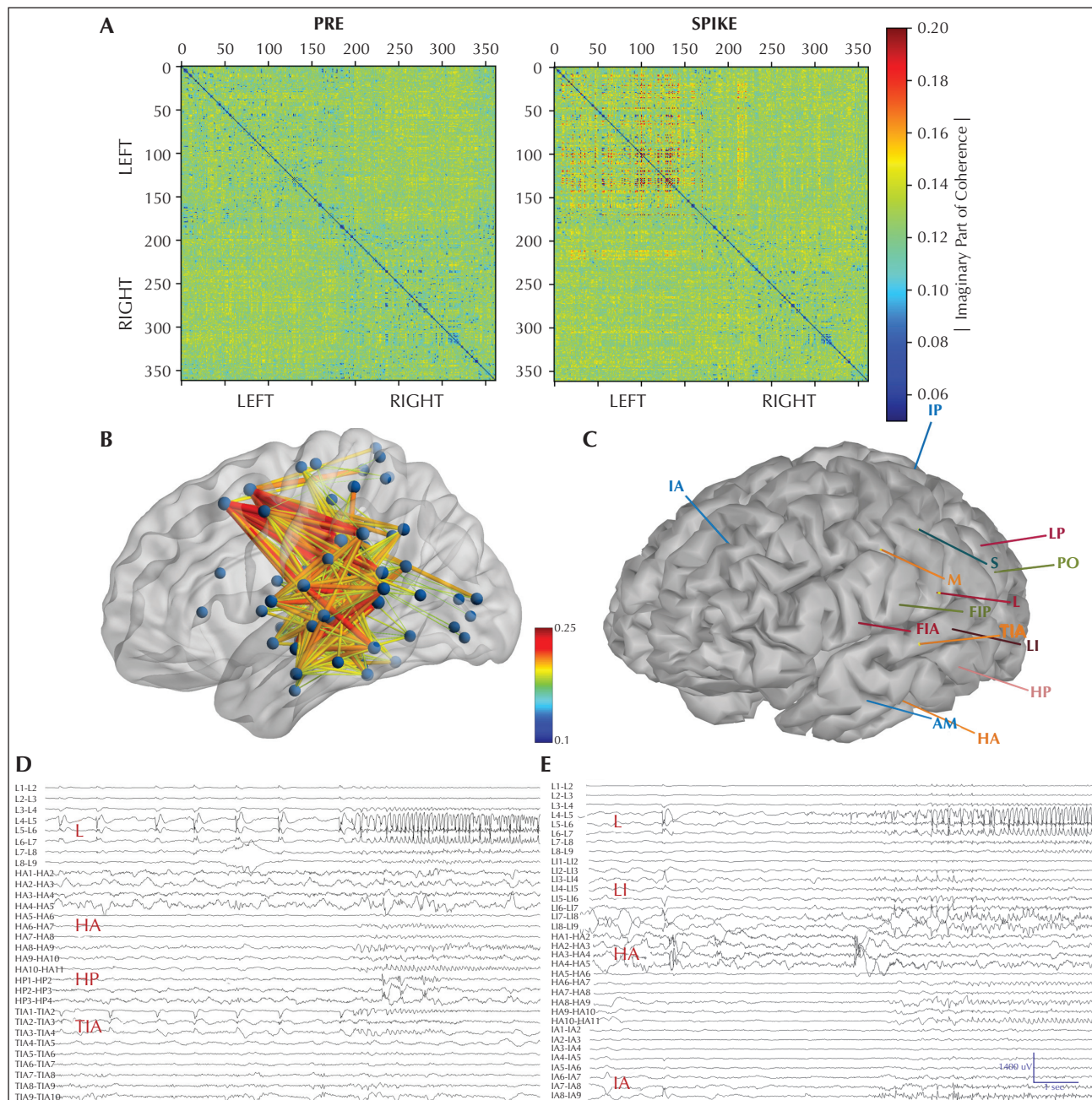
Discussion

This study demonstrates the anatomic correlation between a novel MEG analysis method of non-invasively estimating the epileptic network in epilepsy surgery candidates and subsequent intracranial EEG findings. Even after surgical resection, 20-70% of individuals, depending on their epilepsy type, will continue to have seizures (Malmgren and Edelvik, 2017).

Table 2. EEG, iEEG, and spike-associated network findings.

Subject	EEG spikes	Active areas identified by iEEG*	Anatomic regions in spike-associated network*	Sensitivity (%)
1	Freq. T4	**Interictal: R posterior STG, R posterior Hip, R OFC** Ictal: (a) **R posterior Hip** -> R TOJ); **R posterior STG -> R OFC**, R PCC, R anterior Ins	**R posterior STG, R posterior Hip, R TPOJ, R OFC,** R anterior Hip (<0.001 – 0.012)	**Interictal: 3/3 (1.0)** **Ictal: 3/6 (0.5)**
2	Freq Fp1/F3/F7	**Interictal: L Prec, L TPJ, L OFC,** L IFG **Ictal: L Prec**	**L Prec, L TPJ, L OFC,** L TPOJ, L medial occipital cortex, L posterior MFG, R Prec	**Interictal: 3/4 (0.75)** **Ictal: 1/1 (1.0)**
3	Occ. F7/T3; occ. generalized	**Interictal: L OFC, left medial frontal cortex, left ACC,** L anterior temporal lobe **Ictal: L OFC, L ACC, L medial frontal cortex,** L MTG	**L OFC, L anterior MFG, L** and **R medial frontal cortex, L ACC,** L posterior MFG, L PHC, R antero-lateral temporal lobe, R IFG, R anterior MFG, R frontal Oper, R OFC	**Interictal: 3/4 (0.75)** **Ictal: 3/4 (0.75)**
4	Occ. L and R temporal	**Interictal: L anterior Hip, L TPOJ,** L posterior parietal cortex, R anterior Hip, L posterior Hip **Ictal: L TPOJ, L medial parietal lobe, L TOJ**	**L anterior Hip, L TPOJ, L TOJ, L medial parietal lobe,** L posterior STG, L superior parietal lobe, L IFG, L OFC, R TOJ, R SFG, L visual area V4	**Interictal: 2/5 (0.4)** **Ictal: 3/3 (1.0)**
5	Freq. Fp1, F3, T3	**Interictal: L SMG, L anterior Ins,** L MTG **Ictal: L anterior Ins, L SMG, L STG**	**L SMG, L anterior Ins, L STG, L MTG,** L frontal Oper, L posterior Oper, L posterior Ins, L OFC, R TPOJ, R posterior Oper	**Interictal: 3/3 (1.0)** **Ictal: 3/3 (1.0)**
6	Occ. T3; Occ. Cz	**Interictal: L SMG, L anterior Ins, L amygdala, L posterior Hip, L STG, L posterior SFG,** L lateral parietal lobe, L Prec, L anterior Hip **Ictal: L SMG -> L MTG, posterior SFG**	**L SMG, L anterior Ins, L posterior Hip, L amygdala, L posterior SFG, L MTG, L posterior Ins, L STG**	**Interictal: 7/10 (0.7)** **Ictal: 3/3 (1.0)**

*Bold text indicates areas of overlap between iEEG and spike-associated network findings. EEG: electroencephalography; iEEG: intracranial EEG; R: right; L: left; STG: superior temporal gyrus; MTG: middle temporal gyrus; OFC: orbitofrontal cortex; Hip: hippocampus; TOJ: temporal-occipital junction; TPOJ: temporal-parietal-occipital junction; PCC: posterior cingulate cortex; ACC: anterior cingulate cortex; Prec: precuneus; TPJ: temporal-parietal junction; IFG: inferior frontal gyrus; MFG: middle frontal gyrus; SFG: superior frontal gyrus; Ins: insula; SMG: supramarginal gyrus; Oper: operculum; PHC: parahippocampal cortex.

Figure 1. Representative evaluation and SAN results from Subject 6. (A) Whole-brain connectivity change from the PRE (left) to the SPIKE (right) conditions. Note that the upper left quadrant represents connectivity within the left hemisphere. (B) Significant spike-associated network (*p* < 0 001) with prominent involvement of the left temporo-parietal junction (including supramarginal gyrus), insula, and both medial and lateral temporal lobe (visualization in BrainNetViewer [v1.62, Xia *et al.,* 2013]). (C) 3D brain reconstruction from anatomic T1 MRI with superimposed SEEG electrodes determined from co-registered computed tomography. (D) Intracranial EEG showing interictal spikes in the supramarginal gyrus (L) and insula (deep contacts of TIA); these are followed by a seizure arising in the supramarginal gyrus (L) and rapidly spreading to the lateral temporal lobe (superficial contacts of HA). Polyspikes are also seen in the hippocampus (deep contacts of HP) during the seizure, but these were also seen interictally. (E) Intracranial EEG showing interictal spikes and polyspikes in the supramarginal gyrus (L), the surrounding area (LI), and the anterior hippocampus (deep contacts of HA) followed by a seizure arising in the supramarginal gyrus (L) with rapid spread to surrounding tissue (LI) and the superior frontal gyrus (superficial contacts of IA).

Additionally, 20-30% of potential surgical candidates never undergo resection at all despite extensive presurgical investigations and extended intracranial EEG recordings (Taussig *et al.*, 2014; González-Martínez *et al.*, 2016). In approximately 10% of children undergoing SEEG, the decision not to proceed is due to an inability to identify the epileptogenic zone (McGovern *et al.*, 2019). Both invasive and non-invasive measures of functional connectivity are increasingly used to identify the epileptogenic zone, predict post-operative outcomes, explain surgical failures, and offer new insights into the widespread cognitive effects of focal epilepsies (Murakami *et al.*, 2016; Bear *et al.*, 2019). These methods have not yet, however, reached routine clinical practice due, in part, to a combination of complicated and labor-intensive analyses and limited clinical data.

The SAN method presented here offers some advantages over other approaches of applying functional connectivity to identify epileptic networks. Some of the most promising recent studies use intracranial electrodes to measure functional connectivity and identify the epileptogenic tissue (Lagarde *et al.*, 2018). These studies are limited, however, to the brain areas covered by the intracranial electrode placement. In contrast, MEG is a non-invasive tool capable of studying whole-brain connectivity and is therefore not limited by electrode placement decisions. When considering only brain regions that were included in the SEEG recordings, nodes identified in the SAN were 84% specific for the intracranially-determined epileptic network. Based on these results, one might consider including these nodes during the SEEG planning stages. Additionally, the analytical pipeline can be largely automated, thereby alleviating some of the labor-intensiveness of other approaches. The only steps requiring direct human involvement are the visual identification of spikes for inclusion and co-registration of the MRI and MEG data. Notably, automated approaches to these latter steps are also increasingly feasible (Joshi *et al.*, 2018).

These advantages are similar to another MEG-based method of exploring connectivity patterns related to spikes (Malinowska *et al.*, 2014). In this study, the authors used ICA of MEG recordings to identify spike-containing components, which were then projected into source space. The identified networks showed excellent overlap with the results of their SEEG investigations. In contrast with our method, however, the authors found that the ICA-based networks were generally more anatomically limited than those identified on SEEG. One might expect that the ICA-based approach provides greater specificity and lower sensitivity compared with our method. As such, the preferred method will depend on the goal of the investigation.

In addition to surgical applications, the SAN method could provide novel insights into cognitive deficits associated with focal epilepsies. There is increasing recognition that the cognitive effects of focal epilepsies extend far beyond their foci, suggesting a larger epileptic network than might be expected based solely on the IZ and SOZ (Jehi, 2018; Bear *et al.*, 2019). The broad spike-associated networks described in the present study could provide novel insights into the process underlying the widespread cognitive changes, and further study is warranted to test this possibility.

Some limitations also deserve consideration. The imaginary part of coherence reduces the effects of external noise and spectral leakage, but physiological zero-lag connections, *i.e.* co-varying physiological activity occurring at precisely the same time in multiple areas, are also inherently removed. These zero-lag connections can contain meaningful information (Vicente *et al.*, 2008), and their loss should be balanced with the importance of eliminating spectral leakage and other sources of connectivity artifact. Future application of this technique will require further study and optimization of the network measurement parameters including the most informative frequency bands and the duration of the connectivity estimate time windows. Additionally, the significant SANs consistently overlapped the SEEG-identified IZ and SOZ but also extended well beyond these regions, particularly at lower network thresholds, thereby limiting direct clinical application. A large surgical epilepsy cohort with post-operative outcome data could address these issues by enabling comparison of network features at different computational settings with the clinical outcomes. The workflow could be further enhanced through the use of threshold-free approaches to the NBS, which eliminate the arbitration threshold decisions (Baggio *et al.*, 2018).

Should the technique prove clinically useful, its implementation into the clinical workflow also faces a couple of hurdles. First, significant SANs were most consistently identifiable in individuals with ≥30 spikes, and not all patients will have an adequate spike burden. Second, access to MEG is restricted to a relatively small number of epilepsy centers. High-density EEG, while more computationally complicated, warrants investigation due to its lower cost and potential for longer-duration recordings that could enable capturing more spikes.

Network-based techniques are already helping us understand the network effects of epilepsy. In the future, such techniques, including the SAN presented here, might assist in the presurgical planning stages or even allow smaller resections if we can identify critical hubs in the epileptic network. Additionally, the extensive connectivity changes seen across the brain during spikes could provide new insights into

the widespread cognitive comorbidities associated with focal epilepsy. The SAN results presented in this brief cohort report hint at the underlying potential of this technique to improve our understanding of epilepsy. □

References

Baggio HC, Abos A, Segura B, *et al*. Statistical inference in brain graphs using threshold-free network-based statistics. *Hum Brain Mapp* 2018; 39(6): 2289-302.

Bagić AI, Knowlton RC, Rose DF, Ebersole JS, & ACMEGS Clinical Practice Guideline (CPG) Committee. American Clinical Magnetoencephalography Society Clinical Practice Guideline 1: recording and analysis of spontaneous cerebral activity. *J Clin Neurophysiol* 2011; 28(4): 348-54.

Bear JJ, Chapman KE, Tregellas JR. The epileptic network and cognition: what functional connectivity is teaching us about the childhood epilepsies. *Epilepsia* 2019; 60(8): 1491-507.

Bernhardt BC, Bonilha L, Gross DW. Network analysis for a network disorder: the emerging role of graph theory in the study of epilepsy. *Epilepsy Behav* 2015; 50: 162-70.

Colclough GL, Woolrich MW, Tewarie PK, Brookes MJ, Quinn AJ, Smith SM. How reliable are MEG resting-state connectivity metrics? *Neuroimage* 2016; 138: 284-93.

Engel J. Finally, a randomized, controlled trial of epilepsy surgery. *New Engl J Med* 2001; 345(5): 365-7.

Englot DJ, Hinkley LB, Kort NS, *et al*. Global and regional functional connectivity maps of neural oscillations in focal epilepsy. *Brain* 2015; 138(8): 2249-62.

Glasser MF, Coalson TS, Robinson EC, *et al*. A multi-modal parcellation of human cerebral cortex. *Nature* 2016; 536(7615): 171-8.

González-Martínez J, Bulacio J, Thompson S, *et al*. Technique, results, and complications related to robot-assisted stereoelectroencephalography. *Neurosurgery* 2016; 78(2): 169-80.

Gramfort A, Luessi M, Larson E, *et al*. MEG and EEG data analysis with MNE-Python. *Front Neurosci* 2013; 7: 267.

Jehi L. The epileptogenic zone: concept and definition. *Epilepsy Curr* 2018; 18(1): 12-6.

Jin S-H, Jeong W, Chung CK. Mesial temporal lobe epilepsy with hippocampal sclerosis is a network disorder with altered cortical hubs. *Epilepsia* 2015; 56(5): 772-9.

Joshi CN, Chapman KE, Bear JJ, Wilson SB, Walleigh DJ, Scheuer ML. Semiautomated spike detection software Persyst 13 is noninferior to human readers when calculating the spike-wave index in electrical status epilepticus in sleep. *J Clin Neurophysiol* 2018; 35(5): 370-4.

Sun J, Hong X, Tong S. Phase synchronization analysis of EEG signals: an evaluation based on surrogate tests. *IEEE Trans Biomed Eng* 2012; 59(8): 2254-63.

Lagarde S, Roehri N, Lambert I, *et al*. Interictal stereotactic-EEG functional connectivity in refractory focal epilepsies. *Brain* 2018; 141(10): 2966-80.

Malinowska U, Badier J-M, Gavaret M, Bartolomei F, Chauvel P, Bénar C-G. Interictal networks in magnetoencephalography. *Hum Brain Mapp* 2014; 35(6): 2789-805.

Malmgren K, Edelvik A. Long-term outcomes of surgical treatment for epilepsy in adults with regard to seizures, antiepileptic drug treatment and employment. *Seizure* 2017; 44: 217-24.

McGovern RA, Knight EP, Gupta A, *et al*. Robot-assisted stereoelectroencephalography in children. *J Neurosurg Pediatr* 2019; 23(3): 288-96.

Murakami H, Wang ZI, Marashly A, *et al*. Correlating magnetoencephalography to stereo-electroencephalography in patients undergoing epilepsy surgery. *Brain* 2016; 139(11): 2935-47.

Pascual-Marqui RD. Standardized low-resolution brain electromagnetic tomography (sLORETA): technical details. *Methods Find Exp Clin Pharmacol* 2002; 24(D): 5-12.

Reuter M, Schmansky NJ, Rosas HD, Fischl B. Within-subject template estimation for unbiased longitudinal image analysis. *Neuroimage* 2012; 61(4): 1402-18.

Taussig D, Chipaux M, Lebas A, *et al*. Stereo-electroencephalography (SEEG) in 65 children: an effective and safe diagnostic method for pre-surgical diagnosis, independent of age. *Epileptic Disord* 2014; 16(3): 280-95.

Vicente R, Gollo LL, Mirasso CR, Fischer I, Pipa G. Dynamical relaying can yield zero time lag neuronal synchrony despite long conduction delays. *Proc Natl Acad Sci USA* 2008; 105(44): 17157-62.

Xia M, Wang J, He Y. BrainNet Viewer: a network visualization tool for human brain connectomics. *PLOS One* 2013; 8(7): e68910.

Zalesky A, Fornito A, Bullmore ET. Network-based statistic: identifying differences in brain networks. *Neuroimage* 2010; 53(4): 1197-207.

Zumsteg D, Friedman A, Wieser H, Wennberg R. Propagation of interictal discharges in temporal lobe epilepsy: correlation of spatiotemporal mapping with intracranial foramen ovale electrode recordings. *Clin Neurophysiol* 2006; 117(12): 2615-26.

TEST YOURSELF

(1) What is the role of magnetoencephalography (MEG) in surgical epilepsy?

(2) Is MEG-based functional connectivity useful in surgical epilepsy?

Note: Reading the manuscript provides an answer to all questions. Correct answers may be accessed on the website, www.epilepticdisorders.com, under the section "The EpiCentre".